Supporting Information

69451 Weinheim, Germany

Title Quantifying the solution structure of atomically precise metal nanoclusters using small angle neutron scattering

Xindi Liu, Yuxiang Chen, Ye Yang, Lionel Porcar, Aurel Radulescu, Stefan Guldin, Rongchao Jin,* Francesco Stellacci,* Huayan Yang,* Zhi Luo*

Abstract: Atomically precise metal nanoclusters are a unique class of synthetic material. In contrast to colloidal nanoparticles, their atomic structures can be fully resolved using single crystal X-ray diffraction, and their chemical formula precisely determined by mass spectroscopy. However, obtaining high quality single crystals of these nanoclusters is not a trivial task and their successful ionization in mass spectroscopy remains challenging. Here, we report the application of small angle neutron scattering (SANS) to directly quantify the overall structure parameters of nanoclusters in solution. Adopting a core-shell ellipsoid model, we successfully correlate the scattering patterns of a series of silver and gold nanoclusters with their crystallographic structures. Interestingly, for charged nanoclusters, a discrepancy between the ligand shell thickness from SANS and crystal structures was observed. We attributed such difference to the presence of a layer of counterions in solution. Furthermore, we demonstrate the capability of SANS, when combining with X-ray scattering, in estimating the molecular weight of both the metal core and the ligand shell. This work offers an alternative characterization tool for nanoclusters without the requirement of crystallization or gas phase ionization.

DOI: 10.1002/anie.2021XXXXX

SUPPORTING INFORMATION

Table of Contents

Experimental Procedures

List of figures

Experimental Procedures

S1: synthesis of NCs

Ag_{16}: $AgBF_4$ was dissolved in the mixture of dichloromethane and methanol. DPPE, 3,4-difluorothiophenol, and PPh_4Br were added when the solution was cooled to 0 ℃. After constant stirring for 20 minutes, $NaBH_4$ aqueous solution and triethylamine were then added into mixture under vigorous stirring. The aging process was 12h at 0 ℃. The water phase was removed by syringe and the left mixture in organic phase was washed with water for several times.

Ag_{44}: $AgNO_3$ was dissolved in the mixture of dichloromethane and methanol. 3,4-difluorobenzenethiol and tetraphenylphosphonium bromide were added when the solution was cooled to 0 ℃. After constant stirring for 20 minutes, $NaBH_4$ aqueous solution and triethylamine were then added into mixture under vigorous stirring. The aging process was 12h at 0 ℃. The water phase was removed by syringe and the left mixture in organic phase was washed with water for several times.

Ag_{38}: $AgBF_4$ was dissolved in the mixed solution of dichloromethane and methanol. Triphenylphosphine and 3,4-difluorothiophenol were added into the mixture when it was cooled to 0 ℃ under mild stirring. After 20 minutes, freshly made $NaBH_4$ aqueous solution and triethylamine were added quickly under vigorous stirring. The aging process was taken 12 h at 0 ℃. The water phase was removed by syringe and the left mixture in organic phase was washed with water for several times.

Ag_{63}: $AgBF_4$ was dissolved in the mixed solvent of dichloromethane and methanol. Tributyl phosphine, tetrabutylammonium tetraphenylborate, and 3,4-difluorothiophenol ($HSPhF_2$) were added into the mixture. After 20 minutes, freshly made $NaBH_4$ aqueous solution and triethylamine were added quickly under vigorous stirring when it was cooled to 0 ℃. The aging process was taken 12 h at 0 ℃. The water phase was removed by syringe. The left solution was then centrifugated for 4 minutes at the speed of 10000 rpm. The supernatant was stored frozen in the dark at 4 °C.

Synthesis of the Ag-SPhtBu complex precursor for the following production of Ag_{136} and Ag_{374} NCs: 4-tBuPhSH and NEt_3 were dissolved together in ethanol. The mixture solution was added dropwise into the solution that $AgNO_3$ was dissolved in CH_3CN under stirring for overnight. The solvent was dried and the yellow powder of polymeric Ag-SPhtBu precursor was generated.

Ag_{136} and Ag_{374}: Ag-SPhtBu precursor was added into the mixture of dichloromethane and methanol in a volume ratio of 4:1. PPh_4Br was added when the mixture was cooled to 0 ℃. After 5 minutes constant stirring, freshly made $NaBH_4$ aqueous solution and triethylamine were quickly added under vigorous stirring. The aging process was taken 12 h at 0 ℃. The water phase was removed by syringe and the left mixture in organic phase was washed with water for several times.

Au_{38}: $HAuCl_4 \cdot 3H_2O$ and glutathione (GSH) were dissolved in acetone under vigorous stirring. After 20 minutes, freshly made $NaBH_4$ aqueous solution was added quickly under vigorous stirring when it was cooled to 0 ℃. 20 minutes later, the black precipitates which were $Au_n(SG)_m$ were dissolved by water. Then the aqueous solution of $Au_n(SG)_m$ was mixed with ethanol, toluene, and phenyl ethanethiol. The biphasic solution was heated to 80 ℃ and kept in this temperature. 10 minutes later, the $Au_n(SG)_m$ nanoparticles

were transferred to the organic phase. The heating process was kept for ~ 40 hrs at 80 ℃. $Au_{38}(SCH_2CH_2Ph)_{24}$ nanoparticles were produced after the etching process. The Au NCs were extracted by dichloromethane.

Au_{104}: $HAuCl_4 \cdot 3H_2O$ and tetraoctylammonium bromide (TOABr) were mixed in CH_2Cl_2. After phase transfer and removal of the water layer, phenyl ethanethiol was added in the mixture. 30 minutes later, freshly made $NaBH_4$ aqueous solution was added under vigorously stirring. The following purification was performed by a solvent fractionation.

Au_{144}: $HAuCl_4 \cdot 3H_2O$ and TOABr were added in methanol. Thiols were added in the mixture after 30 minutes vigorous stirring. 15 minutes later, freshly made $NaBH_4$ aqueous solution was added in the mixture. The black precipitates that were washed with methanol to remove excess thiols and were collected by centrifugation. The crude products were dissolved in $CHCl_2$ were pipetted onto multiple pieces of PTLC plates. The developer was the mixture of DCM and petroleum ether. Then the Au_{144} NCs were extracted with pure DCM and tried by rotary evaporation.

S2: SANS measurements

The nanoclusters were recrystallized and the SANS measurements had been performed by dissolving the crystalline powders to assure the purity of the samples. All nanoclusters SANS measurements had been done on D22 at Institut Laue-Langevin except for the measurement of Ag_{44} sample being performed on KWS-2 at Jülich Center for Neutron Science. Measurements were implemented at 25 °C, employing 1.4 m sample-to-detector distance, at 2.8 Å wavelength with a collimation setup of 5.6 m and a q range from 0.04 $Å^{-1}$ to 0.8 $Å^{-1}$. The sample concentration was approximately 10 mg/ml corresponding to a volume fraction of nanocluster solution of below 0.1%. The two-dimensional scattering data were processed and reduced via Grasp software including radial averaging, background subtraction, empty cell, and transmission correction, and normalization to an absolute scale.

S3: SAXS measurements

SAXS measurements had been done on Ganesha 300XL (SAXSLAB) instrument. Borosilicate glass capillaries with inner thickness of 1mm was used for the sample solutions. Roughly, 0.1 mg/ml concentration of the nanocluster solution was used in the measurements.

S4: P(r) analysis and fitting

The P(r) analysis were performed using GNOM software in ATSAS packages. The fitting of the SANS data has been processed through SASview and SASfit software with the core-shell ellipsoid model. The volume of correlation of the SAXS and SANS data was analyzed using Scatter software.

Results and Discussion

Figure S1. The SAXS curve of three AuNCs. The red curve stands for the A_{u38}, while the yellow curve is Au_{104}, and the blue curve is Au_{144}.

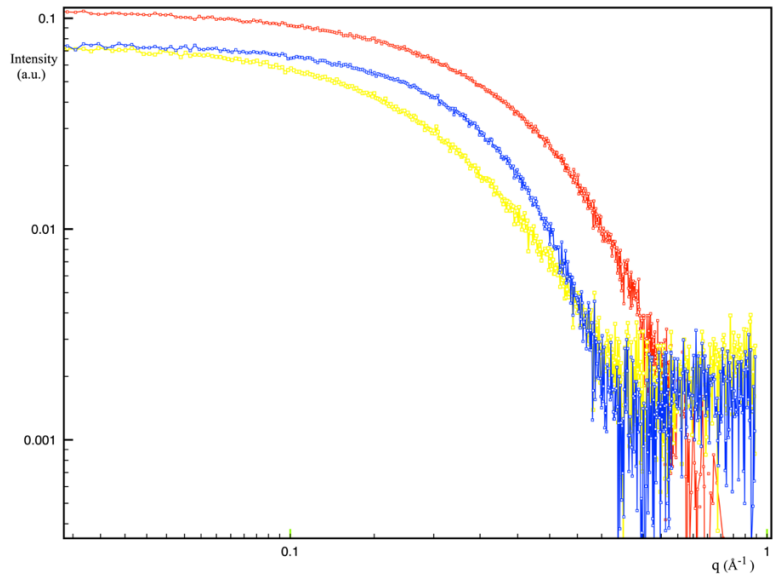

Figure S2. Fitting results of Ag_{16}. (A) fitting data. (B) fitting curve.

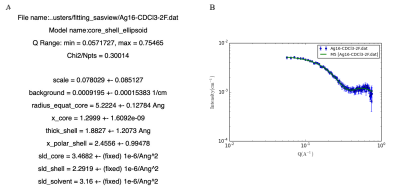

Figure S3. Fitting results of Ag_{38}. (A) fitting data. (B) fitting curve.

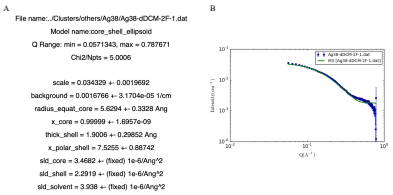

Figure S4. Fitting results of Ag_{44}. (A) fitting data. (B) fitting curve.

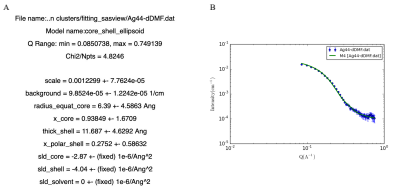

Figure S5. Fitting results of Ag_{63}. (A) fitting data. (B) fitting curve.

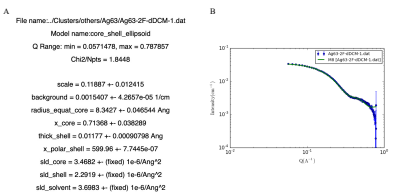

Figure S6. Fitting results of Ag_{136}. (A) fitting data. (B) fitting curve.

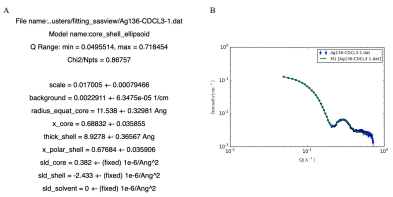

Figure S7. Fitting results of Ag_{374}. (A) fitting data. (B) fitting curve.

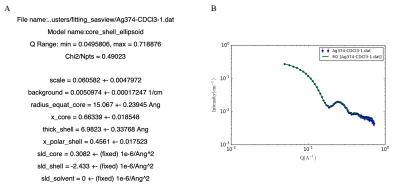

Figure S8. Fitting results of Au_{38}. (A) fitting data. (B) fitting curve.

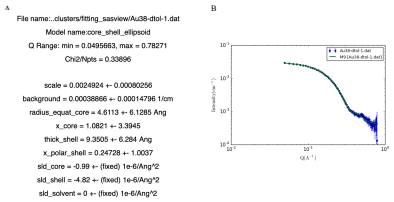

Figure S9. Fitting results of Au_{104}. (A) fitting data. (B) fitting curve.

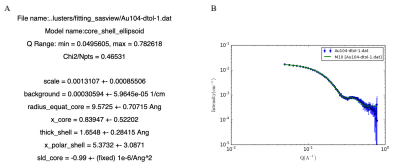

Figure S10. Fitting results of Au_{144}. (A) fitting data. (B) fitting curve.

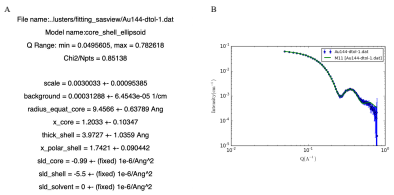

Author Contributions

Xindi Liu and Huayan Yang contributed equally to this work. All authors have given approval to the final version of the manuscript.